

Generalized Logit Adjustment: Improved Fine-tuning by Mitigating Label Bias in Foundation Models

Beier Zhu, Jiequan Cui, Qianru Sun, Hanwang Zhang

Abstract—Foundation models like CLIP allow zero-shot transfer on various tasks without additional training data. Yet, the zero-shot performance is less competitive than a fully supervised one. Thus, fine-tuning and ensembling are also commonly adopted to better fit the downstream tasks. However, we argue that such prior work has overlooked the inherent biases in foundation models. Due to the highly imbalanced Web-scale training set, foundation models are inevitably skewed toward frequent semantics, and thus the subsequent fine-tuning or ensembling is still biased. In this study, we systematically examine the biases in foundation models and demonstrate the efficacy of our proposed Generalized Logit Adjustment (GLA) method. Note that bias estimation in foundation models is challenging, as most pre-train data cannot be explicitly accessed like in traditional long-tailed classification tasks. To this end, GLA offers two alternative methods for debiasing: the first is an optimization-based bias estimation built on Bayes optimal criterion, and the second identifies label bias through an eigenvector derived from a matrix of zero-shot predictions. As our work resolves a fundamental flaw in the pre-training, the proposed GLA demonstrates significant improvements across a diverse range of tasks: it achieves 1.5 pp accuracy gains on ImageNet, a large average improvement (1.9-4.4 pp) on 11 few-shot datasets, 2.4 pp gains on long-tailed classification.

Index Terms—vision-language models, label bias, image classification



1 INTRODUCTION

THANKS to the Web-scale data and self-supervised strategies, foundation models like CLIP [1] empower zero-shot transfer to a wide variety of domains [2]–[4]. However, the zero-shot performance is still weak on several domain-specific tasks such as differentiating models of cars, species of flowers, and variants of aircraft [1], [2]. Therefore, it is a common practice to improve the downstream performance via supervised fine-tuning on labeled data, *e.g.*, linear probing, prompt tuning [5], [6], and end-to-end fine-tuning.

However, fine-tuned models are easily biased: they are adept in exploiting spurious correlations that only hold on the downstream distribution [1], [6]–[8]. To improve the robustness, several studies [6], [8], [9] propose to combine fine-tuned models with zero-shot models. For example, WiSE-FT [8] ensembles the fine-tuned and zero-shot models in weight space and ProGrad [6] uses zero-shot predictions to regularize the fine-tuning gradient. The underlying assumption lies in that the zero-shot models are robust to distribution shifts [1], and their predictions are complementary to those of fine-tuned models [8].

Despite these methods exhibiting performance gains on both in-distribution and out-of-distribution evaluations, they all overlook the inherent bias originating from the foundation models. Specifically, the Web-scale data for pre-training foundation models exhibit a highly skewed distribution due

to Zipf’s law of nature [10]. The resulting foundation models develop a biased decision boundary that leads to a poor zero-shot performance on rare classes. As evidenced in Figure 1(a) and (b), the purple line encounters a dramatic drop, and the zero-shot performance of tail classes is significantly lower than that of head classes (57.2% *vs.* 78.0%). Existing ensemble methods like WiSE-FT [8] overlook the label bias, resulting in an improvement in top-1 (+0.5%) and head accuracy (+1.7%) while a noticeable degradation on the tail performances (−0.9%) in Figure 1(b). Another evidence is that the orange line (WiSE-FT) is below the blue line (fine-tuned models) for rare classes in Figure 1(a).

We propose Generalized Logit Adjustment (GLA), a simple post-hoc method consisting of two steps: **1**) removing the label bias of zero-shot model via estimating the label distribution in the pre-training dataset; **2**) ensembling the fine-tuned and debiased zero-shot models. As illustrated in Figure 1 (b), our GLA achieves consistent improvement across all three subgroups, particularly showing a significant gain on tail classes (+1.5%). Despite its simplicity, our GLA has a firm statistical grounding: it is the Bayes optimal classifier given the fine-tuned and zero-shot models, thus consistent for minimizing the error on a class-balanced target distribution (Section 4.3). It is worth noting that removing the bias of foundation models is challenging since the label distribution is often inaccessible due to privacy or copyright concerns. In this work, we only use the downstream labeled data and the zero-shot model to estimate the foundation label bias, and we propose two distinct methods to achieve this estimation. In our first method, we formulate the problem by adjusting the margin of the zero-shot models such that the lowest error is achieved on the downstream dataset. Method 2 involves constructing a matrix P from the averaged

- B. Zhu, J. Cui, and H. Zhang are with the Department of Computer Science & Engineering, Nanyang Technological University, Singapore.
E-mail: beier002@e.ntu.edu.sg
{jiequan.cui, hanwangzhang}@ntu.edu.sg
- Q. Sun is with the Singapore Management University, Singapore.
E-mail: qianrusun@smu.edu.sg



Fig. 1: (a) Per class accuracy of CLIP-ViT/B16 on ImageNet. Class index are sorted using the estimated pre-training label prior. Curves are smoothed for better visualization. (b) Beak-down performance of different models on ImageNet. We equally divide the ImageNet classes into three subgroups, according to the class index. Existing ensemble methods like WiSE-FT [8] exhibits a clear performance loss on tail classes, while our GLA stands out for all three subgroups.

predicted probability of each class, and then finding the eigenvector of such matrix as the estimated label prior. We prove the non-asymptotic convergence guarantees and demonstrate its better performance over Method 1 in few-shot settings.

The contributions and novelties of this work are summarized as follows:

- We point out the overlooked label bias in foundation models, which originates from the skewness of pre-training distribution that affects the performance of downstream tasks.
- We formalize the estimation of the label bias as a constrained optimization problem (Section 3.2) with theoretical justification (Section 4.2). The entire process does not require access to the pre-training dataset, making it practical for fine-tuning scenarios. We present Generalized Logit Adjustment (GLA) method, which ensembles the debiased zero-shot and fine-tuned models, and demonstrate its superiority over conventional fine-tuning and ensembling by proving it's a Bayes optimal classifier (Section 4.3).
- We build a comprehensive benchmark for evaluation, which considers three real-world settings and three fine-tuning paradigms. The settings are: 1) many-shot learning with abundant data 2) few-shot learning; and 3) long-tail classification, representing a more challenging scenario that combines many-shot and few-shot data (Section 5). The three fine-tuning paradigms include: 1) end-to-end fine-tuning; 2) linear probing; and 3) prompt tuning (Section 3.1).
- We demonstrate the efficacy of our proposed method GLA by conducting extensive experiments across various settings and fine-tuning paradigms. We observe 1 to 1.5 pp accuracy gains on ImageNet, large averaged improvement (1.9 to 4.4 pp) on 11 few-shot datasets and 2.4 pp averaged accuracy gains on long-tail datasets. (Section 5).

This work is an extension of a NeurIPS 2023 paper [11]. Compared to the preliminary manuscript, a more efficient bias estimation method is newly proposed in Section 3.3.2. The justification of the proposed method with convergence analysis are provided in Section 4.2.2. Additional discussions and empirical results that validate the efficacy of the new method are included in Section 5. Our code is publicly

available at <https://github.com/BeierZhu/GLA>.

2 RELATED WORK

Image-text foundation models. Foundation models pre-trained by contrastive objectives have set impressive milestones for image and text representation learning, with CLIP [1], ALIGN [12], CoCa [4] and Flamingo [3] being the exemplars. Such models exhibit impressive prompt-based zero-shot performance on various image recognition downstream tasks. Our method aims to reduce foundation model biases to boost performance in downstream tasks. While [13] also addresses word frequency bias, we differ in two key areas: Firstly, we debias zero-shot models using fixed prompts, whereas [13] refines the prompting process. Secondly, our GLA doesn't require access to a subset of the pre-training data.

Ensembles. Ensemble methods aim to boost performances by combining multiple networks, which can be either implemented by aggregating model outputs [14]–[19], weight-space ensembling [8], [20], or ensemble distillation [21], [22]. For the adaptation of foundation models, several work propose to ensemble the fine-tuned and zero-shot models for better performance: Wortsman et al. [8] ensembles them in weight space; ProGrad and ProReg [6], [9] propose to fuse them via knowledge distillation. Our GLA is orthogonal to these approaches, as it concentrates on mitigating the biases in foundation models that are detrimental to ensemble models.

Logit adjustment. Logit adjustment [23]–[27] is a post-hoc technique to adjust the biased output of classification networks. Kang *et al* [25] proposes an element-wise scaling adjustment for the classifier weight. Tang *et al* [24] removes the projection of features on a global biased direction. Menon [23] derives the theoretically optimal adjustment from the training distribution. Unlike the those approaches which rely on a transparent training data or class distribution, our GLA can eliminate the class bias without accessing to the pre-training statistics.

3 METHODS

3.1 Setup

Task. Consider a classification problem with instances $\mathbf{x} \in \mathcal{X}$ and labels $y \in \mathcal{Y} = [K] = \{1, \dots, K\}$. We have a zero-shot model f_{zs} (given below), a downstream dataset $\mathcal{D}_s =$

$\{\mathbf{x}_i, y_i\}_{i=1}^{N_s}$ drawn from source distribution P_s and a fine-tuned model f_{ft} (given below) trained on the dataset D_s . Give a model $f : \mathcal{X} \rightarrow \mathbb{R}^K$ that outputs prediction score, we define the risk of f on the target distribution \mathbb{P}_t as the mis-classification rate: $\mathcal{R}_t(f) = \mathbb{E}_{\mathbf{x}, y \sim \mathbb{P}_t} [y \neq \text{argmax}_i f(\mathbf{x})_i]$. Our goal is to learn a model f_{gla} that best leverages f_{zs} and f_{ft} that minimizes the risk \mathcal{R}_t .

Zero-shot models. We primarily explore CLIP [1] for zero-shot models. CLIP consists of a visual encoder $\Phi_v(\mathbf{x})$ and a text encoder $\Phi_t(\mathbf{t})$, producing l_2 -normalized features from an image \mathbf{x} and a text \mathbf{t} respectively. Zero-shot model f_{zs} for K classes is enabled by matching image features $\mathbf{v} = \Phi_v(\mathbf{x})$ with classification weights $\mathbf{w}_k = \Phi_t(\mathbf{t}_k)$, where \mathbf{t}_k is obtained by extending the class name $\{c_k\}$ to a pre-defined prompt, e.g., "a photo of a $\{c_k\}$ ". The probability of \mathbf{x} being classified as y is defined as:

$$\mathbb{P}(y|\mathbf{x}) = \text{softmax}(f_{zs}(\mathbf{x}))_y = \frac{\exp(\mathbf{v}^T \mathbf{w}_y)}{\sum_{k=1}^K \exp(\mathbf{v}^T \mathbf{w}_k)}. \quad (1)$$

Fine-tuned models. Standard fine-tuning initializes the model f_{ft} with the pre-trained parameters and then solve $f_{ft} = \text{argmin}_f \mathcal{R}_s(f)$ to minimize the risk on downstream dataset. We consider three common variants of fine-tuning: (1) end-to-end, where all parameters of Φ_v and \mathbf{w}_k are updated; (2) linear probing, where only \mathbf{w}_k is modified while Φ_v is fixed; (3) prompt tuning, where the text input \mathbf{t}_k is learned, while keeping Φ_v and Φ_t frozen.

Notation. Let $\mathbb{P}_p(y)$, $\mathbb{P}_s(y)$ and $\mathbb{P}_t(y)$ be the marginal probability of class $y \in [K]$ for pre-training, source (training) and target (test) distribution, respectively. Let π_p and π_s denote the log probabilities of class for pre-training and training distribution, i.e., $\pi_p(y) = \log \mathbb{P}_p(y)$ and $\pi_s(y) = \log \mathbb{P}_s(y)$.

3.2 Generalized Logit Adjustment Framework

Fine-tuned models often yield significant gains compared to zero-shot models, and ensembling them can further improve performance. This leads to a natural question: How should we best leverage the zero-shot and fine-tuned models for the prediction tasks? We attempt to answer by proposing generalized logit adjustment in Definition 1.

Definition 1. (GLA) The Generalized Logit Adjustment (GLA) model f_{gla} is defined as follows:

$$f_{gla}(\mathbf{x}) = f_{ft}(\mathbf{x}) + f_{zs}(\mathbf{x}) - \pi_s - \pi_p. \quad (2)$$

In Section 4.3, we prove that given the zero-shot and fine-tuned models, our GLA model is the *Bayes* optimal classifier and no other combination of the two models can outperform it. Here remains one important question: how could we obtain π_p as we have no access to the pre-training statistics? We provide the estimation process of π_p in Section 3.3 and postpone the justification in Section 4.2. The entire GLA algorithm consists of two steps which is given as follows:

3.3 Step 1: Estimation of π_p

The first step of our GLA framework is to estimate unknown π_p . We provide two methods, where Method 1 was introduced by us at NeurIPS 2023 [11], and Method 2 is newly proposed in this manuscript. Comparatively, the newly proposed one demonstrates enhanced empirical efficiency with better performance in few-shot setting (Section 5.1), and has non-asymptotic convergence guarantees (Section 4.2.2).

Algorithm 1 Iteration algorithm for solving \mathbf{q}

- 1: **Input:** Matrix P , number of iterations n , tolerance ϵ
 - 2: **Output:** Estimated $\hat{\mathbf{q}}$
 - 3: $\mathbf{q}_0 \leftarrow [\frac{1}{K}, \dots, \frac{1}{K}]$ ▷ initialization
 - 4: **for** $i := 1$ **to** n **do**
 - 5: $\mathbf{q}_i \leftarrow P\mathbf{q}_{i-1}$
 - 6: $\mathbf{q}_i \leftarrow \mathbf{q}_i / \|\mathbf{q}_i\|_1$ ▷ Normalize
 - 7: **if** $\|\mathbf{q}_i - \mathbf{q}_{i-1}\|_1 < \epsilon$ **then** ▷ Check for convergence
 - 8: **break**
 - 9: **end if**
 - 10: **end for**
 - 11: **return** $\hat{\mathbf{q}} \leftarrow \mathbf{q}_i$
-

3.3.1 Method 1: Estimation by solving constrained optimization problem

Let \mathbf{q} be an arbitrary probability simplex over K classes. Given the validation data from \mathbb{P}_t or the balanced training data, we can estimate the $\hat{\pi}_p = \log \hat{\mathbf{q}}$ of the constrained optimization problem (proof in Section 4.2.1):

$$\begin{aligned} \hat{\mathbf{q}} &= \text{argmin}_{\mathbf{q}} \mathcal{R}_t(f_{zs} - \log \mathbf{q}) \\ \text{s.t. } &\mathbf{q}_i \geq 0, \text{ for } i \in [K], \\ &\sum_{i \in [K]} \mathbf{q}_i = 1. \end{aligned} \quad (3)$$

We constrain the sum of \mathbf{q} to be 1 and ensure that each element is non-negative, guaranteeing that it forms a valid probability distribution. We solve the following Lagrangian problem to find optimal $\hat{\mathbf{q}}$:

$$\min_{\mathbf{q}} \max_{\lambda_i \geq 0, v} \mathcal{R}_t(f_{zs} - \log \mathbf{q}) - \sum_i \lambda_i \mathbf{q}_i + v(1 - \sum_{i \in [K]} \mathbf{q}_i). \quad (4)$$

We utilize the optimization toolkit Cooper [28] to implement Eq. (4), where \mathbf{q} is initialized as a uniformed distribution, i.e., $\mathbf{q}(y) = \frac{1}{K}$ for all $y \in [K]$. We use the standard SGD as the primal and dual optimizers for 2000 steps.

3.3.2 Method 2: Estimation by finding stationary distribution

We construct a matrix $P \in \mathbb{R}^{K \times K}$, where each element P_{ij} is computed using downstream dataset as follows:

$$P_{ij} = \frac{1}{N_j} \sum_{\mathbf{x}|Y=j} \text{softmax}(f_{zs}(\mathbf{x}))_i. \quad (5)$$

Then, we can estimate the pre-training label prior \mathbf{q} by solving the following problem:

$$\mathbf{q} = P\mathbf{q} \quad (6)$$

To solve \mathbf{q} , we are essentially looking for the eigenvector \mathbf{v} of P corresponding to the eigenvalue 1 (justification and non-asymptotic guarantee in Section 4.2.2). Interestingly, when regarding P as a transition matrix, the process of estimating \mathbf{q} resembles finding the stationary distribution of a Markov chain. We employ the iterative algorithm described in Algorithm 1 to solve for \mathbf{q} , setting $\epsilon = 10^{-4}$ and $n = 500$ in our implementation.

Despite both methods estimate the pre-training label prior unbiasedly, Section 5.1.2 demonstrates that Method 2 outperforms Method 1 in few-shot scenarios.

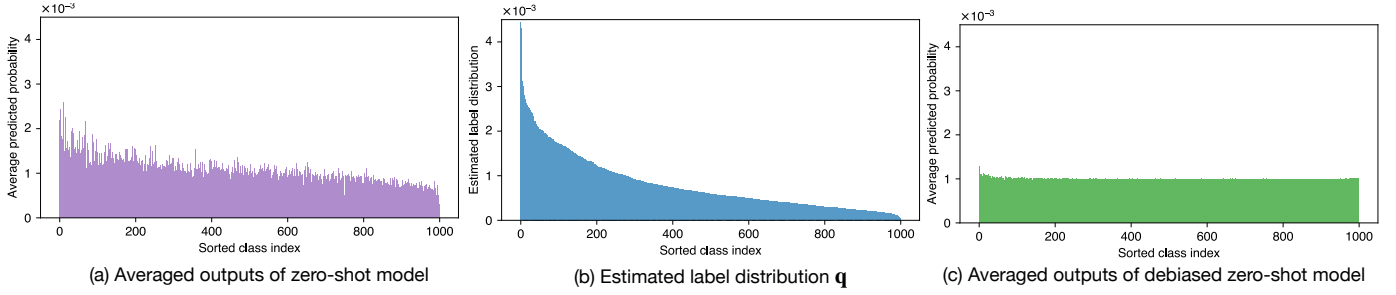


Fig. 2: Illustration of debiasing process on ImageNet validation set. (a) The original distribution of zero-shot outputs; (b) the estimated pre-train distribution \mathbf{q} based on our algorithm; (c) the distribution of debiased zero-shot outputs using estimated \mathbf{q} .

3.4 Step 2: GLA ensembling

Given the estimated $\hat{\pi}_p$ and the known downstream training π_s , we ensemble the zero-shot model f_{zs} and the fine-tuned model f_{ft} to get our GLA model f_{gla} via Eq. (2). We can regard $f_{zs} - \hat{\pi}_p$ and $f_{ft} - \pi_s$ as the debiased zero-shot model (Figure 2(c)) and debiased fine-tuned models, respectively. Our GLA is actually ensembling two debiased models. Note that, different from [6], [8], we *do not* require a hyperparameter to adjust the contribution of the two models, the optimal solution is to combine them equally (see Section 4.3 for justification).

4 THEORETICAL ANALYSIS

In this section, we justify the estimation process of the pre-training label distribution π_p (Section 4.2) and explain why our GLA model best ensembles the zero-shot and fine-tuned models (Section 4.3). We start with some preliminaries on *Bayes* optimal classifier.

4.1 Preliminaries

Suppose we have a pair $(X, Y) \sim \mathbb{P}$ takes values in $\mathcal{X} \times \mathcal{Y}$, where Y is the class label of input X .

Definition 2. The 0-1 error (risk) of a classifier $\hat{y} : \mathcal{X} \rightarrow \mathcal{Y}$ on distribution \mathbb{P} is given by:

$$\mathcal{R}(\hat{y}) = \mathbb{P}(Y \neq \hat{y}(X)) \quad (7)$$

However, the 0-1 error is non-smooth, one typically minimizes a surrogate loss ℓ , e.g., cross-entropy: $\ell(f(\mathbf{x}), y) = \log[\sum_{i \in [K]} \exp(f(\mathbf{x})_i - f(\mathbf{x})_y)]$, where $\hat{y}(\mathbf{x}) = \operatorname{argmax}_i f(\mathbf{x})_i$. It is known that the cross-entropy loss is *Bayes consistent* [29], i.e., a nearly optimal minimizer of the cross-entropy loss ($\mathbb{E}_{\mathbf{x}, y \sim P}[\ell(f(\mathbf{x}), y)]$) is also a nearly optimal optimizer of the mis-classification error ($\mathbb{E}_{\mathbf{x}, y \sim P}[y \neq \hat{y}(\mathbf{x})]$).

Definition 3. The *Bayes optimal classifier* y^* for \mathbb{P} given input \mathbf{x} is defined as:

$$y^*(\mathbf{x}) = \operatorname{argmax}_{y \in \mathcal{Y}} \mathbb{P}(y|\mathbf{x}) \quad (8)$$

It is called *Bayes optimal classifier* because on the average no other classifier using the same hypothesis and prior knowledge can outperform it.

Lemma 1. The *Bayes optimal classifier* y^* for \mathbb{P} has lower risk than all classifiers $\hat{y} : \mathcal{X} \rightarrow \mathcal{Y}$.

$$\mathcal{R}(y^*) \leq \mathcal{R}(\hat{y}) \quad (9)$$

4.2 Estimate the label prior in the pre-training data

We propose two methods to estimate π_p from different perspectives: Method 1 is based on the Bayes optimal criterion, while Method 2 calculates label prior by finding the stationary distribution with a transition matrix P . We will explain these in detail next.

4.2.1 Justification for Method 1

The Method 1 is based on the following proposition that $f_{zs} - \pi_p$ has a lower error on target distribution than any other classifiers that use f_{zs} (see Section 7.1 for the full proof).

Proposition 1. Let $h : \mathbb{R}^K \rightarrow \mathbb{R}^K$ be an arbitrary function that predicts labels using the outputs of the zero-shot model $f_{zs}(\mathbf{x})$. Let the derived classifier be denoted as $f_h(\mathbf{x}) = h(f_{zs}(\mathbf{x}))$. The classifier $f_{zs} - \pi_p$ is better than any $f_h(\mathbf{x})$: $\mathcal{R}_t(f_{zs} - \pi_p) \leq \mathcal{R}_t(f_h(\mathbf{x}))$.

Let \mathbf{q} be an arbitrary probability simplex over K classes, then we have $\mathcal{R}_t(f_{zs}(\mathbf{x}) - \pi_p) \leq \mathcal{R}_t(f_{zs}(\mathbf{x}) - \log \mathbf{q})$. Therefore, we choose to optimize a *probability simplex* \mathbf{q} over K classes such that the model $f_{zs} - \log \mathbf{q}$ achieves the minimal empirical risk, as formulated in Eq. (3) (the Step 1 of GLA algorithm).

4.2.2 Justification for Method 2

We first use the law of total probability to express $\mathbb{P}_p(y)$ and $\mathbb{P}_p(\mathbf{x})$ in Eq. (10) and Eq. (11). Focusing on label shift problem where $\mathbb{P}(\mathbf{x}|y)$ does not change, we derive Eq. (12). By changing the order of integration, we obtain Eq. (13). Since integration can be interpreted as the expectation of a function's value under a certain distribution, we have Eq. (14). Eq. (15) is valid because $\mathbb{P}_p(y')$ is constant w.r.t. to the distribution of \mathbf{x} given y' , it can be move outside

expectation.

$$\mathbb{P}_p(y) = \int_{\mathbf{x}} \mathbb{P}_p(\mathbf{x}) \mathbb{P}_p(y|\mathbf{x}) d\mathbf{x} \quad (10)$$

$$= \int_{\mathbf{x}} \left[\sum_{y' \in \mathcal{Y}} \mathbb{P}_p(\mathbf{x}|y') \mathbb{P}_p(y') \right] \mathbb{P}_p(y|\mathbf{x}) d\mathbf{x} \quad (11)$$

$$= \int_{\mathbf{x}} \sum_{y' \in \mathcal{Y}} \mathbb{P}_s(\mathbf{x}|y') \mathbb{P}_p(y') \mathbb{P}_p(y|\mathbf{x}) d\mathbf{x} \quad (12)$$

$$= \sum_{y' \in \mathcal{Y}} \int_{\mathbf{x}} \mathbb{P}_s(\mathbf{x}|y') \mathbb{P}_p(y') \mathbb{P}_p(y|\mathbf{x}) d\mathbf{x} \quad (13)$$

$$= \sum_{y' \in \mathcal{Y}} \mathbb{E}_{\mathbf{x} \sim \mathbb{P}_s(\mathbf{x}|y')} [\mathbb{P}_p(y') \mathbb{P}_p(y|\mathbf{x})] \quad (14)$$

$$= \sum_{y' \in \mathcal{Y}} \mathbb{P}_p(y') \mathbb{E}_{\mathbf{x} \sim \mathbb{P}_s(\mathbf{x}|y')} [\mathbb{P}_p(y|\mathbf{x})]. \quad (15)$$

Denote $\mathbb{E}_{\mathbf{x} \sim \mathbb{P}_s(\mathbf{x}|y')} [\mathbb{P}_p(y|\mathbf{x})]$ as $\mathbf{p}_{y'}(y)$, we can empirically estimate it from downstream data:

$$\mathbf{p}_{y'}(y) = \mathbb{E}_{\mathbf{x} \sim \mathbb{P}_s(\mathbf{x}|y')} [\mathbb{P}_p(y|\mathbf{x})] \approx \frac{1}{N_{y'}} \sum_{\mathbf{x}|Y=y'} \text{softmax}(f_{zs}(\mathbf{x}))_y, \quad (16)$$

where $N_{y'}$ is the sample size of class y' in downstream dataset. Denote $\mathbf{q}(y) = \mathbb{P}_p(y)$, the Eq. 15 turns into:

$$\mathbf{q}(y) = \sum_{y' \in \mathcal{Y}} \mathbf{p}_{y'}(y) \mathbf{q}(y') \quad (17)$$

Denote $P = [\mathbf{p}_1, \mathbf{p}_2, \dots, \mathbf{p}_K]$ and transform Eq. 17 into matrix formula, we have

$$\begin{bmatrix} \mathbf{q}(1) \\ \mathbf{q}(2) \\ \vdots \\ \mathbf{q}(K) \end{bmatrix} = \begin{bmatrix} \mathbf{p}_1(1) & \mathbf{p}_2(1) & \dots & \mathbf{p}_K(1) \\ \mathbf{p}_1(2) & \mathbf{p}_2(2) & \dots & \mathbf{p}_K(2) \\ \vdots & \vdots & \vdots & \vdots \\ \mathbf{p}_1(K) & \mathbf{p}_2(K) & \dots & \mathbf{p}_K(K) \end{bmatrix} \begin{bmatrix} \mathbf{q}(1) \\ \mathbf{q}(2) \\ \vdots \\ \mathbf{q}(K) \end{bmatrix}, \quad (18)$$

which is precisely Eq. (6).

$$\mathbf{q} = P\mathbf{q} \quad (19)$$

Convergence Analysis. Next, we will explore the sample complexity of our method. Specifically, we aim to bound the absolute error of our estimated label prior when given a confidence level δ and N -shot downstream samples. This is elaborated in the subsequent Proposition (see Section 7.2 for the proof).

Proposition 2. *Suppose we have N -shot downstream samples for K classes. With probability at least $1 - \delta$, the absolute error in \mathbf{q} estimated by method 2 w.r.t. the ℓ_1 norm is:*

$$\|\hat{\mathbf{q}} - \mathbf{q}\|_1 \leq c \cdot \sqrt{\frac{K^2}{2N} \ln \frac{2K^2}{\delta}}, \quad (20)$$

where c is a constant factor.

According to Proposition 2, the error bound for \mathbf{q} decreases with an increasing number of N , following a rate inversely proportional to \sqrt{N} .

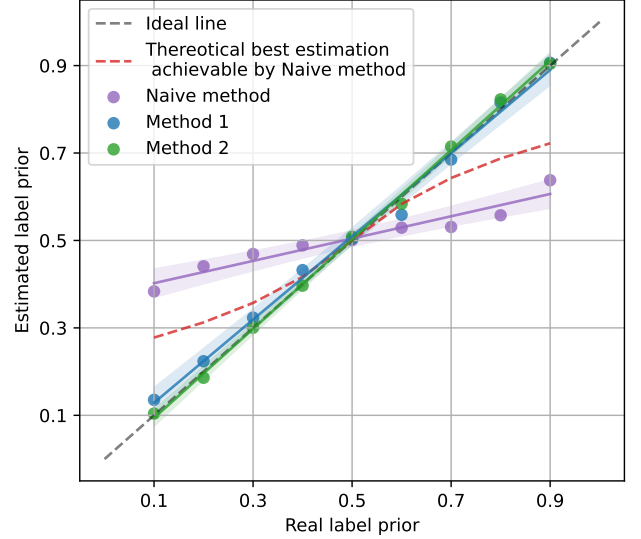


Fig. 3: Evaluation of three label distribution estimation methods.

4.2.3 Further analysis

Allingham et al. [13] propose estimating the label prior by taking the average of zero-shot predictions across a subset of the **pre-training dataset**. We aim to address the following question: *Is it statistically sound to estimate \mathbf{q} by merely averaging the predicted probabilities using **downstream dataset**?* We refer to this approach as the Naive estimation method, and we provide a formal definition below.

Definition 4. (Naive estimation) *The pre-training label prior is estimated by averaging the probabilities that the zero-shot model predicts across the downstream dataset.*

$$\hat{\mathbf{q}}_{\text{naive}} = \mathbb{E}_{\mathbf{x} \sim \mathcal{D}_s} [\text{softmax}(f_{zs}(\mathbf{x}))]. \quad (21)$$

Considering a balanced downstream dataset \mathcal{D}_s , it is obviously that the Naive estimation process is equivalent to

$$\hat{\mathbf{q}}_{\text{naive}} = P \cdot \left[\frac{1}{K}, \dots, \frac{1}{K} \right]^T. \quad (22)$$

Therefore, the Naive method is *not consistent* for estimating the real label prior, which should be represented as $\mathbf{q} = P\mathbf{q}$. Specifically, we consider a binary classification problem to quantify the error estimated by Naive method.

With $K = 2$, we define the truth label prior as $\mathbf{q} = [q, 1 - q]$, where, without loss of generality, we stipulate $q \geq 0.5$. According to Eq. (22), the label prior estimated by Naive method is $\hat{q}_{\text{naive}} = \frac{1}{2}(P_{11} + P_{12})$. It is evident that the error is

$$q - \hat{q}_{\text{naive}} = qP_{11} + (1 - q)P_{12} - \frac{1}{2}(P_{11} + P_{12}) \quad (23)$$

$$= \left(q - \frac{1}{2}\right)(P_{11} - P_{12}) \quad (24)$$

Since $q = qP_{11} + (1 - q)P_{12}$, we get $P_{11} - P_{12} = (q - P_{12})/q$. Combined with Eq. (24), we derive

$$q - \hat{q}_{\text{naive}} = \frac{q - 1/2}{q}(q - P_{12}) \quad (25)$$

We assume that for each class, the averaged predicted probability across samples belonging to that class exceeds

0.5, *i.e.*, $P_{11} > 0.5$ and $P_{22} > 0.5$. This is a conservative assumption, as we would expect a learned model to perform better than random guessing. As $P_{12} + P_{22} = 1$, it is evident that the error in q is at least $q - \hat{q}_{\text{naive}} > \frac{1}{q}(q - 1/2)^2$.

Empirical validation. We conducted an experiment to show that the label priors estimated by Method 1 and 2 closely approximate the actual label prior, whereas the Naive estimation significantly diverges from it. Specifically, we randomly selected two classes from the CIFAR-10 dataset and downsampled the data to obtain different label priors, ranging from 0.1 to 0.9. We then trained a ResNet18 as a biased pre-train model. Finally, we used only the test set to estimate the label prior of the training set. We repeated this process five times and averaged the results for each data point. The results in Figure 3 reveals a strong alignment between the estimation of our proposed method (blue and green line) and the actual label prior (gray dash line). However, the estimation by Naive method (purple line) deviates greatly from the real one. Furthermore, even the best estimation achievable by Naive method (red dash line) still exhibits a large gap ($\frac{1}{q}(q - 1/2)^2$).

The q we estimated is not the marginal probability of the entire pre-training distribution but the label bias matches the downstream distribution. In the above experiment, although training and test sets show different label distributions, their conditional distribution $\mathbb{P}(\mathbf{x}|y)$ remains invariant. In this case, our estimate will converge to the actual training label bias. For CLIP models, with diverse pre-training data, some might not align with the downstream domain, potentially compromising the accuracy of the estimation of the entire pre-training distribution. However, we'd like to point out that removing the label bias of entire pre-training distribution may not optimal for downstream tasks. As a thought experiment, consider a pre-training dataset "sketch" and "photo" styles for "dog" and "cat" samples. Suppose the sample size of "dog" and "cat" is equal but there are more "sketch dogs" than "sketch cats". This means that even if the overall distribution is balanced, each style isn't, resulting in biased zero-shot predictions. if we aim to deploy models for the "sketch dogs and cats" domain, adjusting the overall label bias is insufficient. Instead, the optimal label bias should be estimated on the "sketch" distribution. We also provide experiments using LAION-400M dataset in Section 8.1, illustrating the situation when the downstream data diverges from the pre-training set.

4.3 GLA leads to better ensembling

Zero-shot and fine-tuned models have diverse predictions. We revisit an empirical phenomenon observed in [8] Section 5.1: After exploring a series of measures of diversity, covering predictions and features, they find that zero-shot and fine-tuned models have diverse predictions, despite sharing the same backbone. As the two data distribution P_s and P_p is known to be different, the resulting models leverage different cues to predict: fine-tuned models risk exploiting *spurious correlations and in-domain patterns* which only hold for downstream dataset [30], [31]; On the other hand, zero-shot CLIP models capture *stable correlations* across diverse domains and exhibit much higher robustness [1]. For instance, zero-shot models rely on robust features for decisions that can achieve

high performance on sketch and adversarial samples, while the fine-tuned models that trained on real images typically fail on these samples, as they rely on spurious correlations that only hold on real images. We formulate the phenomena in the following assumption.

Assumption 1. *Zero-shot and fine-tuned models have diverse predictions:*

$$(f_{\text{ft}}(\mathbf{x}) \perp f_{\text{zs}}(\mathbf{x}))|y. \quad (26)$$

We derive the conditional probability $P_t(y|f_{\text{ft}}(\mathbf{x}), f_{\text{zs}}(\mathbf{x}))$ w.r.t. the outputs of $f_{\text{zs}}(\mathbf{x})$ and $f_{\text{ft}}(\mathbf{x})$:

Lemma 2. *For a balanced target distribution¹, where $P_t(y) = 1/K$ for all $y \in [K]$, we have:*

$$\mathbb{P}_t(y|f_{\text{ft}}(\mathbf{x}), f_{\text{zs}}(\mathbf{x})) = \text{softmax}(\underbrace{f_{\text{ft}}(\mathbf{x}) + f_{\text{zs}}(\mathbf{x}) - \pi_s - \pi_p}_{f_{\text{gla}}(\mathbf{x})})(y) \quad (27)$$

Intuitively, since the zero-shot and fine-tuned models provide diverse predictions, conditioned on the two predictions is equivalent to adding the logits in log space. Additionally, as the target distribution is class-balanced, we need to remove the class bias of two models by subtracting π_s and π_p . The formal proof is given in Section 7.3. Note that the RHS of Eq. (27) is exactly the softmax output of our GLA model by Definition 1, which exhibits the following property:

Proposition 3. *Let $g : \mathbb{R}^K \times \mathbb{R}^K \rightarrow \mathbb{R}^K$ be an arbitrary function that ensemble the outputs of f_{zs} and f_{ft} . Our GLA classifier f_{gla} has lower risk than any function $f_g(\mathbf{x}) = g(f_{\text{zs}}(\mathbf{x}), f_{\text{ft}}(\mathbf{x}))$, *i.e.**

$$\mathcal{R}_t(f_{\text{gla}}) \leq \mathcal{R}_t(f_g). \quad (28)$$

Proof. From Lemma 2 and Definition 1, we have:

$$\text{argmax}_{y \in \mathcal{Y}} f_{\text{gla}}(\mathbf{x})_y = \text{argmax}_{y \in \mathcal{Y}} \text{softmax}(f_{\text{gla}}(\mathbf{x}))_y \quad (29)$$

$$= \text{argmax}_{y \in \mathcal{Y}} \mathbb{P}_t(y|f_{\text{ft}}(\mathbf{x}), f_{\text{zs}}(\mathbf{x})), \quad (30)$$

which means f_{gla} is the Bayes optimal classifier (see Definition 3) given $f_{\text{ft}}(\mathbf{x})$ and $f_{\text{zs}}(\mathbf{x})$. According to Lemma 1, any other classifier $g(f_{\text{ft}}(\mathbf{x}), f_{\text{zs}}(\mathbf{x}))$ must have higher risk, *i.e.*, $\mathcal{R}_t(f_{\text{gla}}) \leq \mathcal{R}_t(f_g)$. \square

Proposition 3 demonstrates that our f_{gla} model is the *best* model, as it has the lowest risk on target distribution. Proposition 3 further explains the superiority of f_{gla} over the fine-tuned model f_{ft} and the naive ensemble $f_{\text{ens}}(\mathbf{x}) = f_{\text{ft}}(\mathbf{x}) + f_{\text{zs}}(\mathbf{x})$:

Corollary 1. *f_{gla} performs better than fine-tuned model f_{ft} and naive emsembling f_{ens} :*

$$\mathcal{R}_t(f_{\text{gla}}) \leq \mathcal{R}_t(f_{\text{ft}}), \mathcal{R}_t(f_{\text{gla}}) \leq \mathcal{R}_t(f_{\text{ens}}) \quad (31)$$

Discussion: when do the GLA models degenerate? Note that there are two equality signs in Eq. (31), indicating that the performance of the GLA model can degenerate to be equivalent to that of the fine-tuned model and naive ensembling in the following two cases.

1. This lemma can be easily extended to imbalanced target distributions (proof in Section 7). Yet, as most test sets are class-balanced, we focus on the balanced case for brevity.

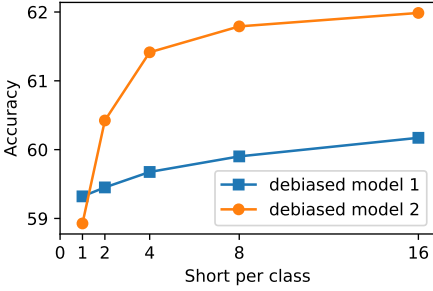


Fig. 4: Performance of two debiased zero-shot models.

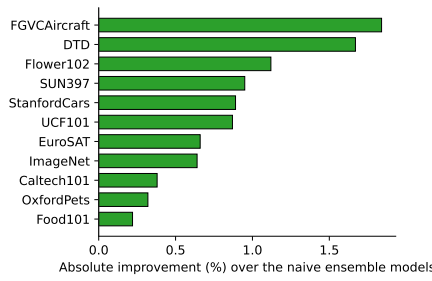


Fig. 5: Comparison with naive ensemble at 16 shots.

Method	Source		Target		
	IN	V2	S	A	R
CLIP	59.8	52.8	35.5	22.8	60.6
CoOp	61.9	54.3	32.5	21.8	54.2
PLOT	63.0	55.1	33.0	21.9	55.6
ProGrad	63.5	55.4	33.1	21.3	55.2
GLA-m2	65.3	56.2	36.5	23.1	61.1

TABLE 1: Evaluation on robustness to distribution shift at 16 training shots.

Model	IN.	Caltech.	Pets.	Cars.	Flowers.	Food.	Aircraft.	SUN.	DTD	EuroSAT	UCF.	Avg.
f_{zs}	59.8	87.1	85.8	55.6	65.3	77.9	17.1	60.3	42.3	37.5	61.5	59.1
$f_{zs} - \hat{\pi}_p^{m1}$	62.3 $\uparrow 2.5$	89.9 $\uparrow 2.7$	85.9 $\uparrow 0.1$	57.6 $\uparrow 2.0$	67.2 $\uparrow 1.9$	78.6 $\uparrow 0.7$	18.4 $\uparrow 1.3$	63.5 $\uparrow 3.2$	43.0 $\uparrow 0.7$	39.0 $\uparrow 1.4$	62.4 $\uparrow 0.9$	60.7 $\uparrow 1.6$
$f_{zs} - \hat{\pi}_p^{m2}$	61.9 $\uparrow 2.1$	90.3 $\uparrow 3.2$	87.3 $\uparrow 1.5$	59.2 $\uparrow 3.6$	68.0 $\uparrow 1.5$	78.6 $\uparrow 2.7$	19.3 $\uparrow 2.2$	63.2 $\uparrow 2.9$	45.5 $\uparrow 3.2$	43.9 $\uparrow 6.4$	64.6 $\uparrow 3.1$	62.0 $\uparrow 2.9$

TABLE 2: Comparison between zero-shot models (f_{zs}) and debiased zero-shot models ($f_{zs} - \hat{\pi}_p$) at 16 shots.

Case 1: For the first equality, if zero-shot model $f_{zs}(\mathbf{x})$ provides no further information about y given $f_{ft}(\mathbf{x})$, i.e., $(y \perp f_{zs}(\mathbf{x}) | f_{ft}(\mathbf{x}))$, then $P_t(y | f_{ft}(\mathbf{x}), f_{zs}(\mathbf{x}))$ degenerates to $P_t(y | f_{ft}(\mathbf{x}))$ and the first equality applies. However, in practice, as downstream model and zero-shot model provides diverse predictions, we usually encounter strict inequality, i.e., $\mathcal{R}_t(f_{gla}) < \mathcal{R}_t(f_{ft})$.

Case 2: The second equality applies when pre-training and downstream training distribution are both class-balanced. In fact, the pre-training dataset for foundation models are known to be highly skewed. Therefore, in most cases, we have $\mathcal{R}_t(f_{gla}) < \mathcal{R}_t(f_{ens})$.

In summary, the above two equalities are usually unattainable, which means that theoretically, our GLA model performs better than both the fine-tuned and the naive ensemble models.

5 EXPERIMENTS

We evaluate our GLA on three real-world scenarios: few-shot (Section 5.1), many-shot (Section 5.2), and long-tail learning (Section 5.3). We show that our GLA boosts performance on all three settings.

5.1 Few-shot learning

5.1.1 Experimental Setup

For few-shot scenarios, we primarily choose prompt tuning for fine-tuning pre-trained models, since it is empirically more effective than end-to-end fine-tuning and linear probing [5], [6], [32].

Datasets. Following CoOp [5], we use 15 datasets for our study: ImageNet [33], Caltech101 [34] for recognizing generic objection, OxfordPets [35]; StanfordCars [36], Flowers102 [37], Food101 [38], FGVCAircraft [39] for fine-grained image classification; EuroSAT [40] for satellite image classification; UCF101 [41] for action recognition; DTD [42] for identifying textures; and SUN397 [43] for scene classification. For domain generalization tasks, we use ImageNet as the source

dataset and select its variants ImageNet-V2 [44], ImageNet-Sketch [45], ImageNet-A [46], ImageNet-R [47] as the target datasets. We randomly select {1, 2, 4, 8, 16} shots for training and use the original test set for evaluation.

Baselines. We compare with three prompt tuning methods: (1) CoOp [5] optimizes prompts via empirical risk minimization; (2) ProGrad [6] prevents forgetting the general knowledge using zero-shot predictions; (3) PLOT [32] applies optimal transport to match the vision and text modalities.

Implementation details. For zero-shot CLIP models, we use prompt ensembling of 80 prompts provided by CLIP [8] for ImageNet and Caltech101 to improve performance, i.e., averaging the text embedding of many captions, e.g., “a photo of a $\{c_k\}$.” and “an image of a $\{c_k\}$.”. For the rest datasets, we use the pre-defined prompt from CoOp [5]. We adopt CLIP-ResNet-50 as the foundation model and adopt class-specific prompt tuning from CoOp. For all few-shot datasets except ImageNet, the training epoch is set to 200 for 16/8 shots, 100 for 4/2 shots, and 50 for 1 shot. For ImageNet, the epoch is set to 50 for all shots. We fine-tune the prompt with SGD optimizer decayed by the cosine annealing rule. The base initial learning rate and batch size are set to 10^{-4} and 32. When given an m -shot sample setting, we increase the learning rate and batch size by m times simultaneously to accelerate the training speed. Results are averaged over three seeds.

5.1.2 Results and analysis

Evaluation of debiased zero-shot models. Figure 4 displays the accuracy of the two debiased models employing Method 1 and Method 2 with varying shots. The Method 2 demonstrates superior debiasing effectiveness in few-shot scenarios. Remarkably, by only adjusting the margin of the zero-shot models, Method 2 can achieve an improvement of nearly 3%. Detailed debiasing results across each dataset at 16 shots are provided in Table 2, where we denote the π_p estimated by Method 1 and Method 2 as $\hat{\pi}_p^{m1}$ and $\hat{\pi}_p^{m2}$, respectively. Both two debiasing methods enhance performance across all 11 datasets. In the following few-shot experiments, we

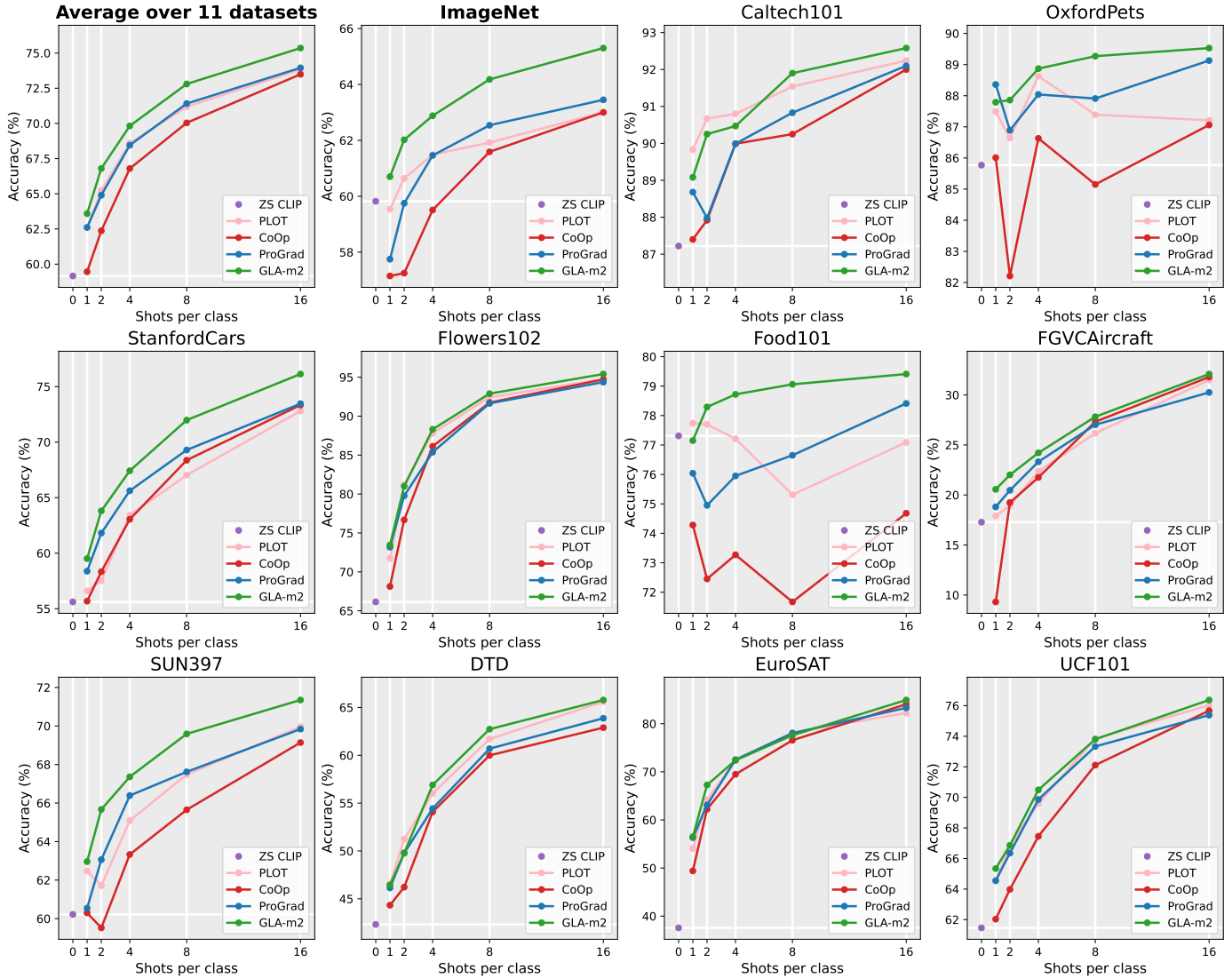


Fig. 6: Accuracy (%) of few-shot learning on 11 datasets.

adopt Method 2 to implement GLA (named as GLA_{-m2}) ensembling due to its efficacy over Method 1.

Compare GLA with baseline methods. Figure 6 summarizes the few-shot results on 11 datasets. Overall, our GLA clearly outperforms the baselines on average performance by a large margin, e.g., our GLA gains 4.1%, 4.4%, 3.0%, 2.8% and 1.9% performance boost over CoOp at 1, 2, 4, 8, 16 shots. In particular, on ImageNet dataset, we observe a large improvement, e.g., 3.0%, 2.3%, 1.4%, 1.6% and 1.9% over ProGrad at 1, 2, 4, 8, 16 shots. Furthermore, on OxfordPerts, Food101 and SUN397 datasets, our method’s performance remains stable and consistently improves with increasing sample sizes, while the one of the baseline methods fluctuates significantly. In particular, on Food101, baseline models even underperform zero-shot models by a large margin, while our GLA shows clearly better performance than zero-shot models.

GLA improves accuracy over naive ensemble. Figure 5 presents a comparison of performance across 11 datasets between our method, GLA_{-m2} , and the naive ensembling approach (defined as $f_{naive}(x) = f_{zs}(x) + f_{ft}(x)$). We rank the

absolute improvements over naive ensembling baseline with a training size of 16 shots. In summary, our GLA_{-m2} demonstrates consistent accuracy gains over the naive ensembling in terms of accuracy gains across all datasets. This highlights how the inherent label bias from pre-training can negatively influence the downstream tasks.

Robustness to distribution shifts. Following CoOp, we used the ImageNet at 16 training shots as the source domain and assess the robustness on ImageNet- $\{V2, Sketch, A, R\}$ datasets. Table 1 summarizes the results, where the prompt tuning baselines perform worse on distribution shifted datasets compared to the zero-shot model, as fine-tuning on limited data misleads the model to learn in-distribution correlations. In comparison, our GLA approach makes the best of both fine-tuned and zero-shot models, thus consistently outperforms other methods on both source and target domains.

5.2 Many-shot learning

5.2.1 Experimental Setup

Datasets. We use ImageNet [33] and CIFAR100 [48] for generic object classification, StanfordCars [36] for fine-

Method	ImageNet		CIFAR100		Stanford Cars		SUN397	
	B/32	B/16	B/32	B/16	B/32	B/16	B/32	B/16
Zero-shot	63.2	68.3	64.2	67.2	59.7	64.4	62.2	64.8
LP	75.8	79.9	80.5	83.1	77.1	83.1	75.6	78.0
E2E	76.3	81.3	89.4	91.0	83.7	90.2	80.0	82.4
WiSE-FT	76.9	81.7	90.0	91.3	84.5	90.7	80.8	82.9
GLA _{-m1}	77.9	82.8	90.7	91.9	85.0	91.1	81.2	83.4
GLA _{-m2}	77.9	82.8	90.8	91.9	85.1	91.0	81.4	83.5

TABLE 3: Accuracy of various methods using CLIP ViT-B/32 and ViT-B/16. Results were obtained using the official implementation from WiSE-FT [8].

grained classification, and SUN397 [43] for scene recognition.

Baselines. We compare GLA against four methods: (1) Zero-shot model, (2) Linear Probing (LP), (3) End-to-End fine-tuning (E2E), and (4) weight ensembling WiSE-FT [8].

Implementation details. We follow WiSE-FT [8] to implement end-to-end fine-tuning. We initialize the classifier with the zero-shot classifier and the output of the image encoder Φ_v is normalized during fine-tuning. We fine-tune for 10 epochs on ImageNet and 20 epochs on other datasets using AdamW [49] optimizer with default hyper-parameters $\beta_1 = 0.9, \beta_2 = 0.999, \epsilon = 10^{-8}$ and weight decay 0.1 and a batch size of 512. We use the same data augmentation and cosine-annealing learning rate schedule as [8]. We denote the GLA models employing Method 1 and Method 2 as GLA_{-m1} and GLA_{-m2}, respectively.

5.2.2 Results and analysis

Main results. Table 3 compares our GLA with various baselines. We observe that GLA_{-m1} and GLA_{-m2} achieve similar results under many shot setting and can increase the performance of end-to-end fine-tuned models: it achieves 1.5% gains on ImageNet. Compared to WiSE-FT, GLA gains 1.1% top-1 accuracy boost on ImageNet dataset. Beyond generic object recognition, our method also improves accuracy on the fine-grained dataset (Stanford Cars) and the scene recognition dataset (SUN397), by 0.4% and 0.5%, respectively.

Breakdown performance analysis. To analyze the impact of pre-training label bias on fine-tuned and ensemble models, we present the breakdown results on ImageNet using CLIP ViT-B/16, as shown in Table 5. Specifically, we sort the class index using the estimated π_p , and assign the top third of the classes as the head classes, the last third as the tail classes, and the remaining classes as the medium classes. Due to the label bias, the zero-shot tail performance is significantly lower than the head one (57.2% vs. 78.0%). The resulting E2E models are also affected by the bias, with the tail performance being 6.3% lower than the head. Existing ensemble WiSE-FT overlooks the bias, exhibiting noticeable degradation on the tail performances (-0.9%) compared to E2E model, while our GLA_{-m1} and GLA_{-m2} stand out for all three subgroups. **Estimated π_p is transferable across different zero-shot models.** The estimated π_p should be transferable across different zero-shot models if they are trained on the same pre-training dataset. To verify this, we employed a CLIP ViT-B/32 based zero-shot model to estimate π_p , which is subsequently used to debias zero-shot models based on CLIP ViT-B/16 and ViT-L/14. As shown in Table 6, our debiased

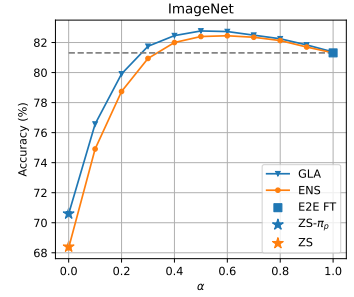


TABLE 4: Accuracy with mixing α .

Method	Head	Med.	Tail	All
Zero-shot	78.0	69.8	57.2	68.3
E2E	83.6	83.0	77.3	81.3
WiSE-FT	85.3	83.7	76.4	81.7
GLA _{-m1}	85.2	84.3	78.8	82.8
GLA _{-m2}	85.3	84.3	78.7	82.8

TABLE 5: Breakdown results on ImageNet.

Model	Source	Target	
	ViT-B/32	ViT-B/16	ViT-L/14
$f_{zs}(\mathbf{x})$	63.2	68.3	75.6
$f_{zs}(\mathbf{x}) - \hat{\pi}_p^{m1}$	65.4	69.3	76.3
$f_{zs}(\mathbf{x}) - \hat{\pi}_p^{m2}$	65.6	69.4	76.4

TABLE 6: Estimated $\hat{\pi}_p$ is transferable across different backbones. $\hat{\pi}_p$ is estimated using CLIP ViT-B/32.

models outperform the original zero-shot versions by a clear margin.

Ensembling with mixing coefficient. In Section 5.2, we prove the optimal solution is to combine the debiased zero-shot and fine-tuned models equally. We now examine the claim by introducing a mixture coefficient $\alpha \in [0, 1]$. The ensemble predictions are given by: $f_{gla}(\mathbf{x}, \alpha) = (1 - \alpha) \cdot (f_{zs}(\mathbf{x}) - \pi_p) + \alpha \cdot (f_{ft}(\mathbf{x}) - \pi_s)$. We compare the GLA_{-m1} and the naive ensembling with mixture α in Figure 4, where GLA_{-m1} meets its optimal performance at $\alpha = 0.5$, which is in line with our theoretical analysis. We also observe that the debiased zero-shot model increases accuracy by 2.3% and our GLA_{-m1} consistently outperforms naive ensembling with various α .

5.3 Long-tail learning

5.3.1 Experimental Setup

Datasets and metrics. We evaluate our method on two standard benchmarks: Places365-LT and ImageNet-LT [50]. In addition to top-1 accuracy, we report the accuracy on three test subsets according to the number of samples per class: many-shot (> 100 samples), medium-shot ($20 \sim 100$ samples), and few-shot (< 20 samples).

Fine-tuning and long-tail learning baselines. We compare our GLA with the combinations of fine-tuning protocols and long-tailed recognition methods. We consider three fine-tuning protocols: 1) Linear Probe (LP); 2) End-to-End (E2E) fine-tuning; 3) Prompt Tuning (PT). We compare with five long-tail learning methods:

	Method	Many	Med	Few	All
LP	ERM	64.4	39.8	20.1	46.6
	LA	56.7	50.5	46.4	52.3
	BS	57.7	50.5	43.9	52.4
	GLA _{-m1}	65.5	60.8	57.7	62.2
	GLA _{-m2}	65.5	60.7	57.6	62.1
PT	ERM	66.6	57.7	53.8	60.6
	LA	67.9	60.0	58.7	62.9
	BS	67.0	62.2	59.4	63.5
	GLA _{-m1}	70.7	66.5	64.3	67.8
	GLA _{-m2}	70.8	66.5	64.4	67.9
E2E	ERM	75.5	56.0	36.2	60.8
	LWS [25]	70.4	62.6	56.2	64.7
	LA [23]	70.4	62.8	56.9	64.9
	BS [51]	71.2	62.5	56.8	65.1
	WiSE-FT [8]	70.7	65.0	61.1	66.7
	BALLAD [52]	71.0	66.3	59.5	67.2
	GLA _{-m1}	72.1	66.4	63.4	68.2
	GLA _{-m2}	72.2	66.3	63.5	68.2

TABLE 7: The performances on ImageNet-LT

	Method	Many	Med	Few	All
LP	ERM	43.9	21.1	9.0	26.9
	LA	39.2	33.7	29.5	34.9
	BS	39.6	34.0	28.3	34.9
	GLA _{-m1}	43.6	40.2	38.8	41.1
	GLA _{-m2}	43.8	40.3	38.8	41.3
PT	ERM	47.7	32.6	24.9	36.5
	LA	43.9	40.6	39.4	41.5
	BS	43.4	42.5	42.3	42.8
	GLA _{-m1}	47.0	47.1	47.8	47.2
	GLA _{-m2}	47.0	47.0	47.9	47.1
E2E	ERM	46.3	27.4	12.5	31.3
	LWS [25]	41.2	39.0	32.8	38.6
	LA [23]	42.2	39.3	34.0	39.3
	BS [51]	46.7	44.4	39.5	44.3
	WiSE-FT [8]	46.0	44.0	43.9	44.7
	BALLAD [52]	48.7	44.7	42.2	45.7
	GLA _{-m1}	47.3	45.4	45.3	46.1
	GLA _{-m2}	47.3	45.5	45.1	46.1

TABLE 8: The performances on Places365-LT

1. Standard ERM: We learn the model by standard empirical risk minimization on the long-tailed data.
2. Learnable Weight Scaling (LWS) [25]: We first learn the model by standard ERM, then fix the model and learn to re-scale the magnitude of the classifier using class-balanced sampling.
3. Logit Adjustment (LA) [23]: We first learn the model by standard ERM, then compensates the long-tailed distribution by subtracting a class-dependent offset to the model outputs.
4. Balanced Softmax (BS) [51] modifies the Softmax cross-entropy loss which explicitly accommodate the label distribution shift during optimization.
5. BALLAD [52] first fine-tunes the vision-language models via contrastive loss on long-tailed data, then freezes the backbone and finally employs an adapter to enhance the representations of tail classes with re-sampling strategies.

Implementation Details. For all combinations of the fine-tuning and long-tail learning baselines, visual backbones are initialized from CLIP-ResNet-50 and all classifiers are initialized by feeding prompt with class names to the text encoder. We use SGD for all experiments with a momentum of 0.9 for 50 epochs with batch size of 512. The initial learning rate is set to 1.6×10^{-3} which is decayed by the cosine annealing rule. To mitigate explosive gradients, we use the warmup learning rate equals to 10^{-5} during the first epoch. For the sake of fairness in comparison, all hyper-parameters of baselines are carefully searched using grid search on the validation set.

5.3.2 Results

Table 8 shows that our GLA method consistently surpasses baselines across all long-tailed datasets. We observe that GLA_{-m1} and GLA_{-m2} achieve similar results on the two benchmarks. Our approach GLA_{-m1} outperforms PT-based models by 3.5% and 4.4% on ImageNet-LT and Places365-LT, respectively. Against E2E approaches, GLA exceeds not just the WiSE-FT but also the current SOTA method BALLAD, by a large margin, e.g., 1% gains on ImageNet-LT.

6 CONCLUSION

In this paper, we identify the label bias in foundation models and underscore its adverse effects on downstream task performance. We propose the Generalized Logit Adjustment (GLA) framework for fine-tuning foundation models, which boosts the performance by effectively eliminating label bias and combining diverse predictions from zero-shot and fine-tuned models. We prove that when presented with zero-shot and fine-tuned models, our GLA is the Bayes optimal classifier for downstream task. Extensive experiments across a diverse range of tasks and fine-tuning framework demonstrate the effectiveness of our approach. We believe that the proposed GLA may partially improve the fairness and credibility of foundation models.

7 PROOFS

7.1 Proof of Proposition 1

Restated Proposition (Proposition 1). *Suppose that the target distribution \mathbb{P}_p is class-balanced. Let $h : \mathbb{R}^K \rightarrow \mathbb{R}^K$ be an arbitrary function that predicts labels using the outputs of the zero-shot model $f_{zs}(\mathbf{x})$. Let the derived classifier be denoted as $f_h(\mathbf{x}) = h(f_{zs}(\mathbf{x}))$. The classifier $f_{zs} - \pi_p$ is better than any $f_h(\mathbf{x})$: $\mathcal{R}_t(f_{zs} - \pi_p) \leq \mathcal{R}_t(f_h(\mathbf{x}))$.*

Proof. Denote the output $\mathbf{z} = f_{zs}(\mathbf{x})$. We first use the Bayes rule to decompose $\mathbb{P}_t(y|\mathbf{z})$ into $\mathbb{P}_t(\mathbf{z}|y)$, $\mathbb{P}_t(y)$ and $\mathbb{P}_t(\mathbf{z})$ in Eq. (32), then consider $\mathbb{P}(\mathbf{z}|y)$ does not change, we derive Eq. (33). Again, using Bayes rule, we have Eq. (34). Since \mathbf{z} is fixed, we replace the term $\frac{\mathbb{P}_p(\mathbf{z})}{\mathbb{P}_t(\mathbf{z})}$ that not rely on y with a constant C_1 in Eq. (35). We replace $\mathbb{P}_p(y) = \exp(\log \mathbb{P}_p(y)) = \exp(\pi_p(y))$ and $\mathbb{P}_t(y) = \exp(\log \mathbb{P}_t(y)) = \exp(\pi_t(y))$. As the underlying class-probabilities $\mathbb{P}_p(y|\mathbf{z}) \propto \exp(\mathbf{z}_y)$ for $y \in [K]$. Denote the constant C_p for normalizing $\exp(\mathbf{z}_y)$ into probability, and merge all constants to $C = \frac{C_1}{C_p}$, we get

Eq. (37). We have Eq. (38) because the summation of $\mathbb{P}_t(y|\mathbf{z})$ is 1, therefore $C = 1/\sum_{i \in [K]} \exp(\mathbf{z} - \pi_p)(i)$.

$$\mathbb{P}_t(y|\mathbf{z}) = \frac{\mathbb{P}_t(\mathbf{z}|y)\mathbb{P}_t(y)}{\mathbb{P}_t(\mathbf{z})} \quad (32)$$

$$= \frac{\mathbb{P}_p(\mathbf{z}|y)\mathbb{P}_t(y)}{\mathbb{P}_t(\mathbf{z})} \quad (33)$$

$$= \mathbb{P}_p(y|\mathbf{z}) \frac{\mathbb{P}_t(y)}{\mathbb{P}_p(y)} \frac{\mathbb{P}_p(\mathbf{z})}{\mathbb{P}_t(\mathbf{z})} \quad (34)$$

$$= C_1 \cdot \mathbb{P}_p(y|\mathbf{z}) \frac{\mathbb{P}_t(y)}{\mathbb{P}_p(y)} \quad (35)$$

$$= \frac{C_1}{C_p} \cdot \exp((\mathbf{z} - \pi_p)(i)) \quad (36)$$

$$= C \cdot \exp((\mathbf{z} - \pi_p)(i)) \quad (37)$$

$$= \exp(\mathbf{z} - \pi_p)(y) / \sum_{i \in [K]} \exp((\mathbf{z} - \pi_p)(i)) \quad (38)$$

$$= \text{softmax}(\mathbf{z} - \pi_p) = \text{softmax}(f_{\mathbf{z}\mathbf{s}}(\mathbf{x}) - \pi_p) \quad (39)$$

Therefore, we have:

$$\operatorname{argmax}_{y \in \mathcal{Y}} (f_{\mathbf{z}\mathbf{s}}(\mathbf{x}) - \pi_p)_y = \operatorname{argmax}_{y \in \mathcal{Y}} \text{softmax}(f_{\mathbf{z}\mathbf{s}}(\mathbf{x}) - \pi_p)_y \quad (40)$$

$$= \operatorname{argmax}_{y \in \mathcal{Y}} \mathbb{P}_t(y|f_{\mathbf{z}\mathbf{s}}(\mathbf{x})) \quad (41)$$

Using Lemma 1, any other classifier $f_h(\mathbf{x})$ has higher risk than $f_{\mathbf{z}\mathbf{s}}(\mathbf{x}) - \pi_p$, i.e., $\mathcal{R}_t(f_{\mathbf{z}\mathbf{s}} - \pi_p) \leq \mathcal{R}_t(f_h(\mathbf{x}))$. \square

7.2 Proof of Proposition 2

Lemma 3. (Hoeffding Inequality) Suppose that X_1, \dots, X_N are N i.i.d bounded random variables, with $0 \leq X_i \leq 1$ for all i . Define $\hat{\mu} = \frac{1}{N} \sum_{i=1}^N X_i$ and let $\mu = \mathbb{E}[X]$, for any $\epsilon > 0$, we have

$$\mathbb{P}(|\hat{\mu} - \mu| > \epsilon) \leq 2 \exp(-2\epsilon^2 N) \quad (42)$$

Lemma 4. (Concentration Inequality for matrix P) Suppose we have N -shot downstream samples for K classes, i.e., $\{\mathbf{x}_n, y_n\}_{n=1}^{N \times K}$. Define $\hat{P}_{ij} = \frac{1}{N} \sum_{\mathbf{x}|Y=j} [\text{softmax}(f_{\mathbf{z}\mathbf{s}}(\mathbf{x}))_i]$ and let $P_{ij} = \mathbb{E}_{\mathbf{x} \sim \mathbb{P}_s(\mathbf{x}|j)} [\text{softmax}(f_{\mathbf{z}\mathbf{s}}(\mathbf{x}))_i]$ for all $i \in [K]$ and $j \in [K]$. With probability at least $1 - \delta$, we have

$$\|\hat{P} - P\|_1 \leq \sqrt{\frac{K^2}{2N} \ln \frac{2K^2}{\delta}} \quad (43)$$

Proof. Using Lemma 3, for any i, j , for any ϵ , we have:

$$\mathbb{P}(|\hat{P}_{ij} - P_{ij}| > \epsilon) \leq 2 \exp(-2\epsilon^2 N) \quad (44)$$

Denote $E = \hat{P} - P$, we observe the following:

$$\left\{ \sum_{i=1}^K |E_{ij}| > \epsilon \right\} \subset \left\{ |E_{1j}| > \frac{\epsilon}{K} \right\} \cup \dots \cup \left\{ |E_{Kj}| > \frac{\epsilon}{K} \right\}. \quad (45)$$

Otherwise, $\sum_{i=1}^K |E_{ij}|$ would be strictly less than ϵ . Then

$$\mathbb{P}\left(\sum_{i=1}^K |E_{ij}| > \epsilon\right) \leq \sum_{i=1}^K \mathbb{P}\left(|E_{ij}| > \frac{\epsilon}{K}\right) \leq 2K \exp(-2\frac{\epsilon^2}{K^2} N) \quad (46)$$

We now turn to bound $\|\hat{P} - P\|_1 = \|E\|_1 = \max_j \sum_{i=1}^K |E_{ij}|$. Considering that

$$\left\{ \max_j \sum_{i=1}^K |E_{ij}| > \epsilon \right\} \subset \left\{ \sum_{i=1}^K |E_{i1}| > \epsilon \right\} \cup \dots \cup \left\{ \sum_{i=1}^K |E_{iK}| > \epsilon \right\}. \quad (47)$$

Otherwise, $\max_j \sum_{i=1}^K |E_{ij}|$ would not be greater than ϵ . Therefore, we have:

$$\mathbb{P}(\|\hat{P} - P\|_1 > \epsilon) = \mathbb{P}\left(\max_j \sum_{i=1}^K |E_{ij}| > \epsilon\right) \quad (48)$$

$$\leq \sum_{j=1}^K \mathbb{P}\left(\sum_{i=1}^K |E_{ij}| > \epsilon\right) \quad (49)$$

$$= 2K^2 \exp(-2\frac{\epsilon^2}{K^2} N) \quad (50)$$

For probability at least $1 - \delta$, let $\delta = 2K^2 \exp(-2\frac{\epsilon^2}{K^2} N)$, the confidence interval $\epsilon = \sqrt{\frac{K^2}{2N} \ln \frac{2K^2}{\delta}}$. \square

Restated Proposition (Proposition 2). Suppose we have N -shot downstream samples for K classes. With probability at least $1 - \delta$, the relative error in \mathbf{q} estimated by Method 2 w.r.t. the ℓ -1 norm is:

$$\|\hat{\mathbf{q}} - \mathbf{q}\|_1 \leq c \cdot \sqrt{\frac{K^2}{2N} \ln \frac{2K^2}{\delta}}, \quad (51)$$

where c is a constant factor.

Proof. First, we introduce the perturbation bounds on the stationary distribution (see Theorem 4.2 [53]): For transition matrix P and $\hat{P} = P + E$ and the stationary distribution \mathbf{q} and $\hat{\mathbf{q}}$, the relation error is bounded by:

$$\|\hat{\mathbf{q}} - \mathbf{q}\|_1 \leq \|EA^\#\|_1, \quad (52)$$

where $A^\#$ is the group inverse of the matrix $A = I - P$.

According to the basic property of matrix norm, we have $\|EA^\#\|_1 \leq \|E\|_1 \|A^\#\|_1$. We set $c = \|A^\#\|_1$ to hide the term that is related to the expected value of P . Using Lemma 4, we arrive at Eq. (52). \square

7.3 Proof of Lemma 2

Restated Lemma (Lemma 2). Let π_t denote the log probability of the target label distribution $\pi_t(y) = \log \mathbb{P}_t(y)$, we have:

$$\mathbb{P}_t(y|f_{\text{ft}}(\mathbf{x}), f_{\mathbf{z}\mathbf{s}}(\mathbf{x})) = \text{softmax}(f_{\text{ft}}(\mathbf{x}) + f_{\mathbf{z}\mathbf{s}}(\mathbf{x}) - \pi_s - \pi_p + \pi_t)(y). \quad (53)$$

In class-balanced target distribution, Eq. (53) simplifies to:

$$\mathbb{P}_t(y|f_{\text{ft}}(\mathbf{x}), f_{\mathbf{z}\mathbf{s}}(\mathbf{x})) = \text{softmax}(f_{\text{ft}}(\mathbf{x}) + f_{\mathbf{z}\mathbf{s}}(\mathbf{x}) - \pi_s - \pi_p)(y). \quad (54)$$

Proof. Denote the output $\mathbf{e} = f_{\text{ft}}(\mathbf{x})$ and $\mathbf{z} = f_{\mathbf{z}\mathbf{s}}(\mathbf{x})$. We first use the Bayes rule to decompose $\mathbb{P}_t(y|\mathbf{e}, \mathbf{z})$ into $\mathbb{P}_t(\mathbf{e}, \mathbf{z}|y)$, $\mathbb{P}_t(y)$ and $\mathbb{P}_t(\mathbf{e}, \mathbf{z})$ in Eq. (55), then rewrite $\mathbb{P}_t(\mathbf{e}, \mathbf{z}|y)$ in Eq. (56) according to Assumption 1. Focusing on label shift

Method	dog	cat	squirrel	tiger	elephant	horse	pig	bird
π_p by [13]	0.059	0.039	0.043	0.053	0.043	0.062	0.061	0.028
π_p by "photo"	0.059	0.041	0.047	0.055	0.048	0.062	0.060	0.033
π_p by "sketch"	0.059	0.043	0.063	0.061	0.067	0.042	0.047	0.056

Method	Sketch	Real Photo
Zero-shot	92.25	97.00
[13]	89.50	97.50
Method 1	93.00	97.75

TABLE 9: Comparison among different bias estimation using Open-CLIP-ViT-B/16.

TABLE 10: Performance on sketch and real photo domain.

problem [23], [27], [54] where $\mathbb{P}(\mathbf{x}|y)$ does not change, we derive Eq. (57)

$$\mathbb{P}_t(y|\mathbf{e}, \mathbf{z}) = \frac{\mathbb{P}_t(\mathbf{e}, \mathbf{z}|y)\mathbb{P}_t(y)}{\mathbb{P}_t(\mathbf{e}, \mathbf{z})} \quad (55)$$

$$= \mathbb{P}_t(\mathbf{e}|y)\mathbb{P}_t(\mathbf{z}|y) \frac{\mathbb{P}_t(y)}{\mathbb{P}_t(\mathbf{e}, \mathbf{z})} \quad (56)$$

$$= \mathbb{P}_s(\mathbf{e}|y)\mathbb{P}_p(\mathbf{z}|y) \frac{\mathbb{P}_t(y)}{\mathbb{P}_t(\mathbf{e}, \mathbf{z})} \quad (57)$$

$$= \frac{\mathbb{P}_s(y|\mathbf{e})\mathbb{P}_s(\mathbf{e})}{\mathbb{P}_s(y)} \frac{\mathbb{P}_p(y|\mathbf{z})\mathbb{P}_p(\mathbf{z})}{\mathbb{P}_p(y)} \frac{\mathbb{P}_t(y)}{\mathbb{P}_t(\mathbf{e}, \mathbf{z})} \quad (58)$$

$$= \frac{\mathbb{P}_s(y|\mathbf{e})}{\mathbb{P}_s(y)} \frac{\mathbb{P}_p(y|\mathbf{z})}{\mathbb{P}_p(y)} \frac{\mathbb{P}_s(\mathbf{e})\mathbb{P}_p(\mathbf{z})\mathbb{P}_t(y)}{\mathbb{P}_t(\mathbf{e}, \mathbf{z})} \quad (59)$$

Since \mathbf{e}, \mathbf{z} are fixed, we can replace the terms that not rely on y with a constant C_1 in Eq. (60). We replace $\mathbb{P}_s(y) = \exp(\log \mathbb{P}_s(y)) = \exp(\pi_s(y))$, $\mathbb{P}_p(y) = \exp(\log \mathbb{P}_p(y)) = \exp(\pi_p(y))$ and $\mathbb{P}_t(y) = \exp(\log \mathbb{P}_t(y)) = \exp(\pi_t(y))$. Suppose the underlying class-probabilities $\mathbb{P}_s(y|\mathbf{e}) \propto \exp(\mathbf{e}_y)$ and $\mathbb{P}_p(y|\mathbf{z}) \propto \exp(\mathbf{z}_y)$ for $y \in [K]$. Denote the constants C_s and C_p for normalizing $\exp(\mathbf{e}_y)$ and $\exp(\mathbf{z}_y)$ into probabilities, and merge all constants to $C = \frac{C_1}{C_s C_p}$, we get Eq. (62)

$$\mathbb{P}_t(y|\mathbf{e}, \mathbf{z}) = \frac{\mathbb{P}_s(y|\mathbf{e})}{\mathbb{P}_s(y)} \frac{\mathbb{P}_p(y|\mathbf{z})}{\mathbb{P}_p(y)} \mathbb{P}_t(y) C_1 \quad (60)$$

$$= \exp(\mathbf{e} + \mathbf{z} - \pi_s - \pi_p + \pi_t)(y) \frac{C_1}{C_s C_p} \quad (61)$$

$$= C \cdot \exp(\mathbf{e} + \mathbf{z} - \pi_s - \pi_p + \pi_t)(y) \quad (62)$$

Because the summation of $\mathbb{P}_t(y|\mathbf{e}, \mathbf{z})$ is 1, $C = 1 / \sum_{i \in [K]} \exp(\mathbf{e} + \mathbf{z} - \pi_s - \pi_p + \pi_t)(i)$. Therefore, we have:

$$\mathbb{P}_t(y|f_{\text{ft}}(\mathbf{x}), f_{\text{zs}}(\mathbf{x})) = \mathbb{P}_t(y|\mathbf{e}, \mathbf{z}) \quad (63)$$

$$= \frac{\exp(\mathbf{e} + \mathbf{z} - \pi_s - \pi_p)_y}{\sum_{i \in [K]} \exp(\mathbf{e} + \mathbf{z} - \pi_s - \pi_p + \pi_t)_i} \quad (64)$$

$$= \text{softmax}(f_{\text{ft}}(\mathbf{x}) + f_{\text{zs}}(\mathbf{x}) - \pi_s - \pi_p + \pi_t)_y \quad (65)$$

In class-balanced target distribution case, $\pi_t = \log \frac{1}{K}$ is constant. Since the softmax function is invariant to constant offsets, Eq. (65) simplifies to:

$$\mathbb{P}_t(y|f_{\text{ft}}(\mathbf{x}), f_{\text{zs}}(\mathbf{x})) = \text{softmax}(f_{\text{ft}}(\mathbf{x}) + f_{\text{zs}}(\mathbf{x}) - \pi_s - \pi_p)_y \quad (66)$$

□

8 ADDITIONAL EXPERIMENTS

8.1 Experiments on LAION-400M

To support our thought experiment in the discussion of Section 4.2, we use the Open-CLIP ViT-B/16 [55], the first 20k image in LAION-400M datasets and the bias estimation

method proposed by [13] to estimate the expected logits across 8 classes: "dog", "cat", "squirrel", "tiger", "elephant", "horse", "pig" and "bird". The bias estimation proposed by [13] provides a good estimation of $\log \mathbb{P}(\mathbf{x})$ over the labels under pre-training distribution. Our GLA estimates the label bias matches the downstream domain, we consider two downstream domain styles, *i.e.*, "photo" and "sketch" from DomainNet [56] dataset. For each domain, we randomly sampled 50 images for each class.

We present the expected logits estimated by [13], along with the one calculated from "photo" and "sketch" downstream domain data in Table 9. Since the softmax is invariant to constant offsets, *i.e.*, $\text{softmax}(\mathbf{x} + c) = \text{softmax}(\mathbf{x})$, we align the three label bias to yield the same logits on "dog" class by subtracting constant values. We observe that the label bias estimated by the "photo" domain align closely with [13] due to its close resemblance to the pre-trained domain. Conversely, the "sketch" image style, which significantly differs from the pre-training domain, results in a more pronounced deviation in the pre-trained label bias.

Additionally, we apply the three estimated label biases to debias the zero-shot model and evaluate the classification performance. The results are shown in Table 10, where the superiority of our method becomes evident on "sketch" domain (93.00% vs 92.25%). Applying the label bias from [13] on the "sketch" domain degrades the model's performance (from 92.25% to 89.50%). This is attributed to the overall pre-training label bias does not adequately reflect the bias specific to the "sketch" domain.

ACKNOWLEDGMENTS

This research is supported by the National Research Foundation, Singapore under its AI Singapore Programme (AISG Award No: AISG2-PhD-2021-01-002 and AI Singapore AISG2-RP-2021-022).

REFERENCES

- [1] A. Radford, J. W. Kim, C. Hallacy, A. Ramesh, G. Goh, S. Agarwal, G. Sastry, A. Askell, P. Mishkin, J. Clark *et al.*, "Learning transferable visual models from natural language supervision," in *ICML*, 2021.
- [2] T. B. Brown, B. Mann, N. Ryder, M. Subbiah, J. Kaplan, P. Dhariwal, A. Neelakantan, P. Shyam, G. Sastry, A. Askell, S. Agarwal, A. Herbert-Voss, G. Krueger, T. Henighan, R. Child, A. Ramesh, D. M. Ziegler, J. Wu, C. Winter, C. Hesse, M. Chen, E. Sigler, M. Litwin, S. Gray, B. Chess, J. Clark, C. Berner, S. McCandlish, A. Radford, I. Sutskever, and D. Amodei, "Language models are few-shot learners," in *NeurIPS*, 2020.
- [3] J.-B. Alayrac, J. Donahue, P. Luc, A. Miech, I. Barr, Y. Hasson, K. Lenc, A. Mensch, K. Millican, M. Reynolds *et al.*, "Flamingo: a visual language model for few-shot learning," in *NeurIPS*, 2022.
- [4] J. Yu, Z. Wang, V. Vasudevan, L. Yeung, M. Seyedhosseini, and Y. Wu, "Coca: Contrastive captioners are image-text foundation models," *TMLR*, 2022.
- [5] K. Zhou, J. Yang, C. C. Loy, and Z. Liu, "Learning to prompt for vision-language models," *IJCV*, 2022.

- [6] B. Zhu, Y. Niu, Y. Han, Y. Wu, and H. Zhang, "Prompt-aligned gradient for prompt tuning," in *ICCV*, 2023.
- [7] H. Pham, Z. Dai, G. Ghiasi, K. Kawaguchi, H. Liu, A. W. Yu, J. Yu, Y.-T. Chen, M.-T. Luong, Y. Wu *et al.*, "Combined scaling for zero-shot transfer learning," *arXiv preprint arXiv:2111.10050*, 2021.
- [8] M. Wortsman, G. Ilharco, J. W. Kim, M. Li, S. Kornblith, R. Roelofs, R. G. Lopes, H. Hajishirzi, A. Farhadi, H. Namkoong *et al.*, "Robust fine-tuning of zero-shot models," in *CVPR*, 2022.
- [9] B. Zhu, Y. Niu, S. Lee, M. Hur, and H. Zhang, "Debiased fine-tuning for vision-language models by prompt regularization," *AAAI*, 2023.
- [10] W. J. Reed, "The pareto, zipf and other power laws," *Economics letters*, 2001.
- [11] B. Zhu, K. Tang, Q. Sun, and H. Zhang, "Generalized logit adjustment: Calibrating fine-tuned models by removing label bias in foundation models," in *NeurIPS*, 2023.
- [12] C. Jia, Y. Yang, Y. Xia, Y.-T. Chen, Z. Parekh, H. Pham, Q. Le, Y.-H. Sung, Z. Li, and T. Duerig, "Scaling up visual and vision-language representation learning with noisy text supervision," in *ICML*, 2021.
- [13] J. U. Allingham, J. Ren, M. W. Dusenberry, X. Gu, Y. Cui, D. Tran, J. Z. Liu, and B. Lakshminarayanan, "A simple zero-shot prompt weighting technique to improve prompt ensembling in text-image models," in *ICML*, 2023.
- [14] T. G. Dietterich, "Ensemble methods in machine learning," in *Multiple Classifier Systems: First International Workshop*, 2000.
- [15] E. Bauer and R. Kohavi, "An empirical comparison of voting classification algorithms: Bagging, boosting, and variants," *Machine learning*, 1999.
- [16] B. Lakshminarayanan, A. Pritzel, and C. Blundell, "Simple and scalable predictive uncertainty estimation using deep ensembles," *NeurIPS*, 2017.
- [17] Y. Freund and R. E. Schapire, "A decision-theoretic generalization of on-line learning and an application to boosting," *Journal of computer and system sciences*, 1997.
- [18] A. Kumar, T. Ma, P. Liang, and A. Raghunathan, "Calibrated ensembles can mitigate accuracy tradeoffs under distribution shift," in *UAI*. PMLR, 2022.
- [19] X. Yi, J. Deng, Q. Sun, X.-S. Hua, J.-H. Lim, and H. Zhang, "Invariant training 2d-3d joint hard samples for few-shot point cloud recognition," in *ICCV*, 2023.
- [20] P. Izmailov, D. Podoprikin, T. Garipov, D. Vetrov, and A. G. Wilson, "Averaging weights leads to wider optima and better generalization," *UAI*, 2018.
- [21] G. Hinton, O. Vinyals, and J. Dean, "Distilling the knowledge in a neural network," *NeurIPS Workshop*, 2014.
- [22] T. Lin, L. Kong, S. U. Stich, and M. Jaggi, "Ensemble distillation for robust model fusion in federated learning," in *NeurIPS*, 2020.
- [23] A. K. Menon, S. Jayasumana, A. S. Rawat, H. Jain, A. Veit, and S. Kumar, "Long-tail learning via logit adjustment," in *ICLR*, 2021.
- [24] K. Tang, J. Huang, and H. Zhang, "Long-tailed classification by keeping the good and removing the bad momentum causal effect," *NeurIPS*, 2020.
- [25] B. Kang, S. Xie, M. Rohrbach, Z. Yan, A. Gordo, J. Feng, and Y. Kalantidis, "Decoupling representation and classifier for long-tailed recognition," in *ICLR*, 2020.
- [26] T. Wu, Z. Liu, Q. Huang, Y. Wang, and D. Lin, "Adversarial robustness under long-tailed distribution," *CVPR*, 2021.
- [27] Y. Hong, S. Han, K. Choi, S. Seo, B. Kim, and B. Chang, "Disentangling label distribution for long-tailed visual recognition," in *CVPR*, 2021.
- [28] J. Gallego-Posada and J. Ramirez, "Cooper: a toolkit for Lagrangian-based constrained optimization," 2022.
- [29] T. Zhang, "Statistical behavior and consistency of classification methods based on convex risk minimization," *The Annals of Statistics*, 2004.
- [30] R. Taori, A. Dave, V. Shankar, N. Carlini, B. Recht, and L. Schmidt, "Measuring robustness to natural distribution shifts in image classification," *NeurIPS*, 2020.
- [31] M. Arjovsky, "Out of distribution generalization in machine learning," Ph.D. dissertation, New York University, 2020.
- [32] G. Chen, W. Yao, X. Song, X. Li, Y. Rao, and K. Zhang, "Prompt learning with optimal transport for vision-language models," *ICLR*, 2023.
- [33] J. Deng, W. Dong, R. Socher, L.-J. Li, K. Li, and L. Fei-Fei, "Imagenet: A large-scale hierarchical image database," in *CVPR*, 2009.
- [34] L. Fei-Fei, R. Fergus, and P. Perona, "Learning generative visual models from few training examples: An incremental bayesian approach tested on 101 object categories," in *CVPRW*, 2004.
- [35] O. M. Parkhi, A. Vedaldi, A. Zisserman, and C. Jawahar, "Cats and dogs," in *CVPR*, 2012.
- [36] J. Krause, M. Stark, J. Deng, and L. Fei-Fei, "3d object representations for fine-grained categorization," in *CVPRW*, 2013.
- [37] M.-E. Nilsback and A. Zisserman, "Automated flower classification over a large number of classes," in *Indian Conference on Computer Vision, Graphics & Image Processing*, 2008.
- [38] L. Bossard, M. Guillaumin, and L. Van Gool, "Food-101—mining discriminative components with random forests," in *ECCV*, 2014.
- [39] S. Maji, E. Rahtu, J. Kannala, M. Blaschko, and A. Vedaldi, "Fine-grained visual classification of aircraft," *arXiv preprint arXiv:1306.5151*, 2013.
- [40] P. Helber, B. Bischke, A. Dengel, and D. Borth, "Eurosat: A novel dataset and deep learning benchmark for land use and land cover classification," *IEEE Journal of Selected Topics in Applied Earth Observations and Remote Sensing*, 2019.
- [41] K. Soomro, A. R. Zamir, and M. Shah, "Ucf101: A dataset of 101 human actions classes from videos in the wild," *arXiv preprint arXiv:1212.0402*, 2012.
- [42] M. Cimpoi, S. Maji, I. Kokkinos, S. Mohamed, and A. Vedaldi, "Describing textures in the wild," in *CVPR*, 2014.
- [43] J. Xiao, J. Hays, K. A. Ehinger, A. Oliva, and A. Torralba, "Sun database: Large-scale scene recognition from abbey to zoo," in *CVPR*, 2010.
- [44] B. Recht, R. Roelofs, L. Schmidt, and V. Shankar, "Do imagenet classifiers generalize to imagenet?" in *ICML*, 2019.
- [45] H. Wang, S. Ge, Z. Lipton, and E. P. Xing, "Learning robust global representations by penalizing local predictive power," *NeurIPS*, 2019.
- [46] D. Hendrycks, K. Zhao, S. Basart, J. Steinhardt, and D. Song, "Natural adversarial examples," in *CVPR*, 2021.
- [47] D. Hendrycks, S. Basart, N. Mu, S. Kadavath, F. Wang, E. Dorundo, R. Desai, T. Zhu, S. Parajuli, M. Guo *et al.*, "The many faces of robustness: A critical analysis of out-of-distribution generalization," in *CVPR*, 2021.
- [48] A. Krizhevsky, "Learning multiple layers of features from tiny images," University of Toronto, Tech. Rep., 2009.
- [49] I. Loshchilov and F. Hutter, "Decoupled weight decay regularization," in *ICLR*, 2019.
- [50] Z. Liu, Z. Miao, X. Zhan, J. Wang, B. Gong, and S. X. Yu, "Large-scale long-tailed recognition in an open world," in *CVPR*, 2019.
- [51] J. Ren, C. Yu, X. Ma, H. Zhao, S. Yi *et al.*, "Balanced meta-softmax for long-tailed visual recognition," *NeurIPS*, 2020.
- [52] T. Ma, S. Geng, M. Wang, J. Shao, J. Lu, H. Li, P. Gao, and Y. Qiao, "A simple long-tailed recognition baseline via vision-language model," *arXiv preprint arXiv:2111.14745*, 2021.
- [53] C. D. Meyer, Jr, "The condition of a finite markov chain and perturbation bounds for the limiting probabilities," *SIAM Journal on Algebraic Discrete Methods*, vol. 1, no. 3, pp. 273–283, 1980.
- [54] Z. Lipton, Y.-X. Wang, and A. Smola, "Detecting and correcting for label shift with black box predictors," in *ICML*, 2018.
- [55] G. Ilharco, M. Wortsman, R. Wightman, C. Gordon, N. Carlini, R. Taori, A. Dave, V. Shankar, H. Namkoong, J. Miller, H. Hajishirzi, A. Farhadi, and L. Schmidt, "Openclip," Zenodo, Tech. Rep., jul 2021.
- [56] X. Peng, Q. Bai, X. Xia, Z. Huang, K. Saenko, and B. Wang, "Moment matching for multi-source domain adaptation," in *ICCV*, 2019.

9 BIOGRAPHY SECTION

Beier Zhu received the B.S. and M.Eng. degrees in electrical engineering from Tsinghua University, China. He is currently pursuing the Ph.D. degree with the School of Computer Science and Engineering, Nanyang Technological University, Singapore. His research interests include foundation models and out-of-distribution generalization.

Jiequan Cui received the Ph.D. degree at the Chinese University of Hong Kong (CUHK). He is currently a Research Fellow at Nanyang Technological University. His research interests include model generalization, neural architecture search, adversarial robustness, imbalanced learning, and image segmentation.

Qianru Sun received the Ph.D. degree from Peking University in 2016. She is an assistant professor of computer science at the School of Computing and Information Systems, at Singapore Management University. Her research interests include Meta Learning, Continual Learning, Causality, Image Generation and Semantic Segmentation.

Hanwang Zhang received the BEng degree in computer science from Zhejiang University, China, in 2009, and the PhD degree in computer science from the National University of Singapore in 2014. He is currently an associate professor with Nanyang Technological University, Singapore. He was a research scientist with the Department of Computer Science, Columbia University, USA. His research interests include computer vision, multimedia, and social media. Dr. Zhang was the recipient of the Best Demo Runner-Up Award in ACM MM 2012, Best Student Paper Award in ACM MM 2013, Best Paper Honorable Mention in ACM SIGIR 2016, and TOMM Best Paper Award 2018. He was the winner of the Best PhD Thesis Award of the School of Computing, National University of Singapore, 2014.

Dear Editors,

Our submission “Generalized Logit Adjustment: Improved Fine-tuning by Mitigating Label Bias in Foundation Models” to TPAMI is an extension of our conference paper published at NeurIPS 2023. The changes are intensive, as summarized in the following.

Change 1: We introduce a more efficient method for addressing label bias in foundation models, as detailed in Section 3.3.2. This novel method stands in stark contrast to the approach outlined in the original manuscript, which relied on a *Bayes* optimal criterion. Our method innovatively represents label bias as a function of the average predicted probabilities across classes. This approach is not only statistically robust but is also substantiated with comprehensive justification and convergence analysis, which we elaborate on in Section 4.2.2.

Change 2: We present new analysis and comparison among three different label bias estimation methods, *i.e.*, Naive estimation, Method 1 and Method 2, in Section 4.2.3. We prove that merely taking the average of zero-shot predictions using downstream dataset is not consistent for estimating the real label prior: for binary classification problem, the error in label prior estimated by Naive method is at least $\frac{1}{q}(q - \frac{1}{2})^2$, where q is the real label prior. This discovery is further validated by experiments on CIFAR10 dataset, where the estimation by Naive method deviates greatly from the real one.

Change 3: We have developed a comprehensive benchmark for evaluating the efficacy of our newly proposed bias estimation method, detailed in Section 5. This benchmark is designed to reflect diverse real-world scenarios, encompassing few-shot, many-shot, and long-tail learning, and incorporates three fine-tuning paradigms: linear probing, prompt-tuning, and end-to-end fine-tuning. Obvious improvements are observed on the benchmark:

(I) On few-shot learning, the improvements are yielded across 15 datasets when equipped prompt tuning with our GLA framework. The Method 2 demonstrates superior debiasing effectiveness over the original method, *e.g.*, Method 2 gains 1.3% averaged accuracies boost over the original method at 16 shots.

(II) In the context of many-shot learning, our approach, referred to as GLA-m2, achieves 1.5% accuracy gains on ImageNet datasets, and shows consistent better performance over naive ensembling. Furthermore, the estimated label bias is transferable across different models, *e.g.*, label bias estimated by Method 2 with CLIP-ViT-B/32 can enhance the accuracy of ViT-B/16 by 1.1% on the ImageNet dataset, showcasing its model-agnostic transferability.

(III) On long-tail learning, our GLA model method consistently surpasses the baselines across the ImageNet-LT and Places365-LT datasets. For PT-based framework, our approach GLA-m2 outperforms baselines by 5.0% and 5.6% on ImageNet-LT and Places365-LT, respectively. Against E2E approaches, GLA exceeds not just the WiSE-FT but also the current SOTA method BALLAD, by a large margin, *e.g.*, 1% gains on ImageNet-LT dataset.

We respectfully submit the manuscript for your consideration for publication.

Best regards,

Beier Zhu